

BLACK HOLE HYPERACCRETION INFLOW-OUTFLOW MODEL II. SHORT AND LONG-SHORT GAMMA-RAY BURSTS AND “QUASI-SUPERNOVAE”

CUI-YING SONG, TONG LIU AND ANG LI

Department of Astronomy, Xiamen University, Xiamen, Fujian 361005, China

ABSTRACT

The detections of some long gamma-ray bursts (LGRBs) relevant to mergers of neutron star (NS)-NS or black hole (BH)-NS, as well as some short gamma-ray bursts (SGRBs) probably produced by collapstars, muddle the boundary of two categories of gamma-ray bursts (GRBs). In both cases, a plausible candidate of central engines is a BH surrounded by a hyperaccretion disk with strong outflows, launching relativistic jets driven by Blandford-Znajek mechanism. In the framework of compact binary mergers, we test the applicability of the BH hyperaccretion inflow-outflow model on powering observed GRBs. We find that, for a low outflow ratio, $\sim 50\%$, postmerger hyperaccretion processes could power not only all SGRBs but also most of LGRBs. Some LGRBs might do originate from merger events in the BH hyperaccretion scenario, at least on the energy requirement. Moreover, kilonovae might be produced by neutron-rich outflows, and their luminosities and timescales significantly depend on the outflow strengths. GRBs and their associated kilonovae are competitive with each other on the disk mass and total energy budgets in our model. The stronger the outflow, the more similar the characteristics of kilonovae to supernovae (SNe). This kind of ‘nova’ might be called ‘quasi-SN’.

Keywords: accretion, accretion disks - black hole physics - gamma-ray burst: general - magnetic fields
- stars: neutron

1. INTRODUCTION

Gamma-ray bursts (GRBs) are classified into two categories divided by $T_{90} \sim 2$ s, i.e., long- and short-duration GRBs (LGRBs and SGRBs, see e.g., Kouveliotou et al. 1993). It is well known that SGRBs are possibly originated from the mergers of neutron star (NS)-NS or black hole (BH)-NS (e.g., Paczyński 1986; Eichler et al. 1989; Paczyński 1991; Popham et al. 1999; Narayan et al. 1992; Berger 2014), and LGRBs associated with type Ib/c supernovae (SNe) could be powered by collapsars (e.g., Tutukov et al. 1992; Galama et al. 1998; Hjorth et al. 2003; Stanek et al. 2003; Woosley & Bloom 2006; Campana et al. 2006; Fruchter et al. 2006; Kumar & Zhang 2015). With the accumulation of observational data, some LGRBs, such as GRB 060614 (e.g., Gehrels et al. 2006; Zhang et al. 2007b, 2009), were found to be relevant to mergers, while some SGRBs such as GRB 090426 (e.g., Antonelli et al. 2009; Levesque et al. 2010; Xin et al. 2011) were produced probably by collapsars. Those bursts muddle the LGRB-SGRB boundary. Zhang et al. (2009) summarized the nature of GRBs and proposed a new classification

approach mainly based on their progenitors.

Two types of GRB central engines have been widely discussed: hyper-accreting stellar mass BHs (e.g., Woosley 1993; Lei et al. 2009, 2013; Liu et al. 2017a) and rapidly spinning and highly magnetized NSs (magnetars, see e.g., Usov 1992; Thompson 1994; Dai & Lu 1998; Zhang & Mészáros 2001; Dai et al. 2006). The detection of gravitational waves (GWs) from close compact binary mergers (e.g., Eichler et al. 1989; Schutz 1989; Cutler & Flanagan 1994; Lipunov et al. 1997; Abadie et al. 2010) provides a direct way to verify the progenitors of SGRBs if the association of GWs with SGRBs can be confirmed. After merger events, optical/near-infrared (NIR) emission from the radioactive decay of heavy r-process elements are produced by the merger remains. These transient events are named ‘kilonovae’ (Li & Paczyński 1998). Recently, the NS-NS merger GW event (GW170817) was detected by the LIGO/Virgo collaboration (e.g., Abbott et al. 2017a; Abbott et al. 2017b; Alexander et al. 2017; Blanchard et al. 2017; Hallinan et al. 2017; Troja et al. 2017; Shappee et al. 2017). Its electromagnetic counterpart, GRB 170817A accompanied by a kilonova AT2017gfo, was also discovered (e.g., Abbott et al. 2017c; Chornock et al. 2017; Cowperthwaite et al. 2017; Evans et al. 2017; Kilpatrick et al. 2017; Margutti et al.

2017; Nicholl et al. 2017; Smartt et al. 2017). This event provides the first direct evidence for the progenitor hypothesis of SGRBs.

Outflows might be present in accretion processes, especially for super-Eddington accretion disks (e.g., Shakura & Sunyaev 1973). They were widely studied by theoretical analyses (e.g., Blandford & Begelman 1999; Liu et al. 2008; Gu 2015), numerical simulations (e.g., Eggum et al. 1988; Okuda 2002; Ohsuga et al. 2005; Ohsuga & Mineshige 2011; Jiang et al. 2014, 2017; McKinney et al. 2014; Sądowski et al. 2014; Sądowski & Narayan 2015), as well as observations (e.g., Wang et al. 2013; Cheung et al. 2016; Parker et al. 2017a). Narayan & Yi (1994) proposed that the advection-dominated accretion flows (ADAFs) with the positive Bernoulli parameter might generate outflows and, by extension, jets (e.g., Narayan & Yi 1995; Abramowicz et al. 1995). Blandford & Begelman (1999) emphasized the roles of the outflows in ADAFs and developed a variant named advection-dominated inflow-outflow solution (ADIOS). They also constructed 1D and 2D self-similar solutions and found that the structure and radiation of flows were subject to the outflows (Blandford & Begelman 2004). As to the study of the vertical structures of the disks, strong outflows were required in both optically-thick and optically-thin flows, resulted from energy equilibrium (e.g., Gu & Lu 2007; Gu 2015). Outflows might also exist in neutrino-dominated accretion flows (NDAFs, see reviews by Liu et al. 2017a). Liu et al. (2012a) visited the vertical structures and luminosities of NDAFs. They found that outflows might be present in the outer region of the disks, depending on the vertical distributions of the Bernoulli parameter.

A wide variety of mechanisms could lead to the generation of outflows. In optically-thick accretion flows, photons could exert radiation pressure upon materials to blow them away. For the optically-thin cases, such as ADAFs, they might possess a positive Bernoulli parameter due to their high internal energy (Narayan & Yi 1994; Gu 2015). Moreover, the Blandford-Payne process (Blandford & Payne 1982) could produce outflows for both optically-thin and optically-thick disks (e.g., Ma et al. 2017).

Apart from theoretical studies, several simulation results also implied that outflows might play essential roles in accretion systems. It was first pointed out by Stone et al. (1999), where 2D hydrodynamic numerical simulations were carried out. Many later simulations confirmed their conclusion, for example in Hawley et al. (2001), Machida et al. (2001), Igumenshchev et al. (2003), Pang et al. (2011), and Yuan & Narayan (2014). Furthermore, both the inflow and outflow mass accretion rates decreased inward, fol-

lowing a power-law $\dot{M} \propto r^s$ ($0 \leq s \leq 1$). For the outflows, $s \approx 1$ was possible which means that more than 90% of the materials could be pushed into powerful outflows from the accretion disk (e.g., Yuan et al. 2012a,b; Begelman 2012). In the global 3D radiation magneto-hydrodynamical simulation, Jiang et al. (2014) found that the radiation-driven outflows were formed along the rotation axis and about 20% of the radiative energy were carried by outflows. In a recent study of super-Eddington accretion flows onto supermassive BHs (SMBHs), the outflow speed could approach $\sim 0.1 - 0.4 c$, and the mass flux lost could reach 15% – 50% of the net mass accretion rates (Jiang et al. 2017). The 3D general-relativistic magnetohydrodynamic simulations of NDAFs indicated that the velocities of powerful outflows likely approached $\sim 0.03 - 0.1 c$ (e.g., Siegel & Metzger 2017).

Recent observations also showed the importance of outflows in accretion systems. For Galactic SMBH accretion, more than 99% original gas escaped from the disk (Wang et al. 2013). In quiescent galaxies, Cheung et al. (2016) observed that centrally-driven winds could suppress the star formation. The ultrafast outflow of the Seyfert I galaxy IRAS 13224-3809 was discovered by Parker et al. (2017a). They also proposed that the outflows could be detected from the long-term X-ray variability (Parker et al. 2017b). Furthermore, the observed kilonova following GRB 130603B (Berger et al. 2013a; Tanvir et al. 2013) might also related to disk winds (e.g., Metzger & Fernández 2014).

Outflows play the important roles in the BH accretion processes, however, few studies have been done on the BH hyperaccretion system. To investigate the nature of the GRB central engine, we necessarily confront the BH hyperaccretion inflow-outflow model with observational data. In paper I, we constrained the characteristics of the progenitor stars of LGRBs and Ultra-LGRBs with the BH hyperaccretion inflow-outflow model in the collapsar scenario (Liu et al. 2017c). In the present work, the applicability of the model is tested to power both SGRBs and LGRBs in the compact binary merger scenario. We further examine the properties of kilonovae triggered by strong neutron-rich outflows. The paper is organized as follows. In Section 2, we describe our BH hyperaccretion inflow-outflow model. The GRB data are presented in Section 3. The properties of kilonovae are shown in Section 4. Section 5 is a brief summary.

2. MODEL

A hyperaccreting stellar mass BH may form just after the mergers of NS-NS or BH-NS. The neutrino annihilation process (e.g., Popham et al. 1999; Di Matteo et al. 2002; Narayan et al. 2001; Liu et al. 2007) and the Blandford-Znajek (BZ) mechanism

(Blandford & Znajek 1977; Blandford & McKee 1977; Lee et al. 2000a,b) are possible ways to power GRBs. Some studies have shown that BZ mechanism is more efficient than the neutrino annihilation (e.g., Kawanaka et al. 2013; Liu et al. 2015a; Lei et al. 2017). Here we assume that the relativistic jets are driven by BZ mechanism, then the BZ jet power can be estimated as

$$L_{\text{BZ}} = 9.3 \times 10^{53} a_*^2 \dot{m}_{\text{in}} X(a_*) \text{ erg s}^{-1} \quad (1)$$

and

$$X(a_*) = F(a_*) / (1 + \sqrt{1 - a_*^2})^2, \quad (2)$$

where $F(a_*) = [(1+q^2)/q^2][(q+1/q) \arctan(q) - 1]$ with $q = a_*/(1 + \sqrt{1 - a_*^2})$. $a_* \equiv cJ_{\text{BH}}/GM_{\text{BH}}^2$ is the dimensionless spin parameter of the BH. M_{BH} and J_{BH} are the mass and angular momentum of the BH.

After compact binary mergers, only a fraction of remaining materials forms an accretion disk around the BH, due to the distribution of the orbital angular momentum. We adopt λ to denote this ratio. m_{re} stands for the dimensionless residual mass in solar mass, and f represents the ratio of the outflow mass to the disk mass. As mentioned in the Introduction, outflows have been found to be very strong in many studies, therefore we take $f = 99\%$ for the strongest outflow case, and $f = 50\%$ as a typical value for comparison. The dimensionless net accretion rate is defined as

$$\dot{m}_{\text{in}} = \frac{f\lambda m_{\text{re}}}{T_{90,\text{rest}}} \quad (3)$$

where $T_{90,\text{rest}} = T_{90}/(1+z)$ is the gamma-ray duration in the rest frame of the source, and z stands for the redshift.

Recently, the simulations of NS-NS mergers (e.g., Dietrich et al. 2015) and BH-NS mergers (e.g., Foucart et al. 2014; Just et al. 2015; Kyutoku et al. 2015; Kiuchi et al. 2015; Siegel & Metzger 2017) showed that the remnant disk mass m_{re} likely possessed an upper limit $\sim 0.3 M_{\odot}$, which depends on the equation of state of the NS, the mass ratio, the total mass and the period of the binary (e.g., Oechslin & Janka 2006; Dietrich et al. 2015). We therefore take $m_{\text{re}} = 0.01, 0.1, 0.3$ in our calculations.

On the other hand, the jet power can be obtained from the observational data of GRBs (e.g., Fan & Wei 2011; Liu et al. 2015b; Song et al. 2016), i.e.,

$$L_{\text{j}} \simeq \frac{(E_{\gamma,\text{iso}} + E_{\text{k,iso}})(1+z)\theta_{\text{j}}^2}{T_{90}}, \quad (4)$$

where $E_{\gamma,\text{iso}}$, $E_{\text{k,iso}}$, and θ_{j} denote the isotropic radiated energy, the isotropic kinetic energy of afterglows, and the jet opening angle, respectively.

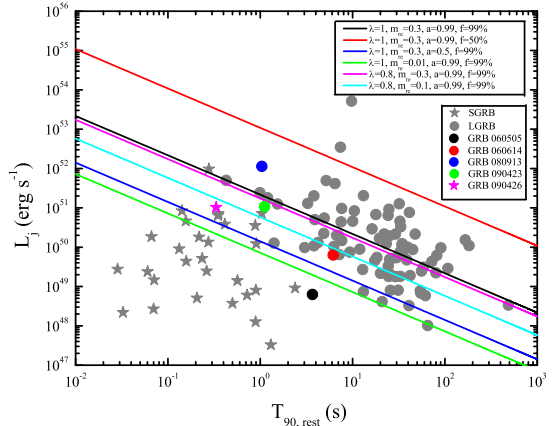


Figure 1. Luminosities and timescales of BZ jets originated from compact binary mergers in six solid lines, different colors corresponding to different parameters as labelled. The gray filled stars and circles denote SGRBs and LGRBs data, respectively. The magenta star stands for SGRB that may be related to the collapse of massive stars. The colorful circles are for LGRBs possibly from NS-NS or BH-NS mergers.

3. GRB DATA

As shown in Table 1, we collected the data of T_{90} , z , $E_{\gamma,\text{iso}}$, $E_{\text{k,iso}}$, θ_{j} and the peak energy in the rest frame $E_{\text{p,rest}}$ of 30 SGRBs and 89 LGRBs. It is worth noting that the measurements of $E_{\gamma,\text{iso}}$, $E_{\text{k,iso}}$, and θ_{j} are model dependent. Considerable debates surround the origins of some GRBs due to their perplexing observational phenomena (e.g., Zhang et al. 2009; Xin et al. 2011; Kann et al. 2011; Li et al. 2016), some unusual GRBs are labelled by the superscript * in the table, which are shown as following:

GRB 060505 This burst has a duration of 4 ± 1 s, the low energy $\sim 10^{49}$ erg and a very low redshift $z = 0.0894$. The presence of a SN is ruled out down to limit of hundreds times fainter than SN 1998bw (Ofek et al. 2007; Fynbo et al. 2006). The star formation rate, metallicity, ionization state of the host environment are more similar to SGRBs than to LGRBs (Levesque & Kewley 2007).

GRB 060614 Its $T_{90} \sim 100$ s in the BAT (15–150 keV) band groups it with LGRBs, while its peak luminosity and temporal lag completely satisfy the SGRB subclass (Gehrels et al. 2006). The low-star-formation-rate host galaxy (Savaglio et al. 2009), and its irrelevant to any known SN (Gal-Yam et al. 2006; Fynbo et al. 2006; Della Valle et al. 2006) suggest that it is related to a compact binary merger rather than a collapsar (e.g., Zhang et al. 2007a). Furthermore, the discovery of a NIR bump in afterglow denotes the strong connection between GRB 060614 and a kilonova, and provides tangible evidence to support the merger origin (Yang et al. 2015; Jin et al. 2015; Horesh et al. 2016).

GRB 080913 The burst duration T_{90} in the BAT

band is 8 ± 1 s. Considering its high redshift $z = 6.7$, the rest-frame duration of this burst is $T_{90,\text{rest}} \sim 1$ s. Pal'Shin et al. (2008) fitted the Konus-Wind and the *Swift*/BAT joint spectral analysis, and derived that the best fit peak energies are $E_{\text{peak}} = 131_{-48}^{+225}$ keV and $E_{\text{peak}} = 121_{-39}^{+232}$ keV for the cutoff power law and Band-function spectra, respectively. Placing this GRB at $z = 1$, it can be classified as SGRBs due to intrinsically short duration and hard spectrum. Pérez-Ramírez et al. (2010) presented the X-ray, NIR and millimetre observations, and proposed that the progenitor of this burst was likely from a BH-NS merger. A maximally-rotating BH might form in the center and power this GRB by the BZ mechanism. However, this GRB is consistent with the lag-luminosity correlation and the Amati relation of LGRBs, which makes the collapsar origin cannot be ruled out (Greiner et al. 2009; Zhang et al. 2009).

GRB 090423 Similar to GRB 080913, this burst was measured with a high redshift $z = 8.6$ and a BAT band duration $T_{90} = 10.3 \pm 1.1$ s. In rest frame, the peak energy and duration are 491 ± 200 keV (Amati et al. 2009) and ~ 1.1 s, respectively.

GRB 090426 It is a SGRB with an observed duration of $T_{90} \sim 1.28$ s at $z = 2.609$ (Antonelli et al. 2009). On the other hand, the soft spectrum $E_{\text{p,rest}} = 177_{-65}^{+90}$ keV (Amati et al. 2009) and burst environment are similar to those of LGRBs. The number density of the medium ($> 11.2 \text{ cm}^{-3}$) is not consistent with the condition of the compact-binary-merger progenitors, which often occur in low density medium (e.g., Xin et al. 2011).

Above all, the observed LGRBs and SGRBs are contaminated by each other. Some studies also found that the duration distributions of SGRBs and LGRBs overlapped each other (e.g., Horváth 2002). Certainly T_{90} is not a good criterion to manifest the nature of GRBs, which resulted in the old dichotomy between the LGRBs related to collapsars and the SGRBs originated from compact binary mergers.

Figure 1 shows the luminosities and timescales of the BZ jets originated from the compact binary mergers. The solid lines in different colors correspond the BZ jets with the different values of λ , m_{re} , a_* , and f . The gray filled stars and circles denote SGRBs and LGRBs data, respectively. The magenta star stands for the SGRB

which may related to the collapse of massive stars. The colorful circles are for LGRBs possibly from NS-NS or BH-NS mergers. By comparing the red and black lines, one can find that the luminosities of SGRBs decrease when the outflow increases. For $f = 50\%$, most of LGRBs find their place under our predicted lines of the BZ jets produced by the BH hyperaccretion inflow-outflow model in the framework of the compact binary mergers. For $f = 99\%$, at least half of those LGRBs cannot be explained by our model. Therefore, our model can explain not only all SGRBs but also most of LGRBs (with a low outflow ratio).

Actually, assuming that T_{90} is near or proportional to the duration of the central engine activity, then the duration of GRBs may be closely related to the properties of progenitors. The collapsar scenario is suggested to produce LGRBs through accretion because of the typical envelope fallback timescale is 10 s (e.g., MacFadyen & Woosley 1999). The BH accretion disk systems after NS-NS/BH-NS mergers have a typical accretion timescale $\sim 0.01 - 0.1$ s, which were raised to account for SGRBs in many models (e.g., Narayan et al. 2001; Aloy et al. 2005). However, the discover of X-ray flares (e.g., Burrows et al. 2005; Nousek et al. 2006; Wu et al. 2007; Chincarini et al. 2010; Margutti et al. 2010; Mu et al. 2016a,b), extended emission (e.g., Lazzati et al. 2001; Connaughton 2002; Norris et al. 2010, 2011; Liu et al. 2012b) and plateaus (e.g., Troja et al. 2007; Rosswog 2007; Rowlinson et al. 2013) in some GRBs denote that the duration of the GRB central engine activity is much longer than T_{90} in both LGRBs and SGRBs. The gamma-ray duration T_{90} may much shorter than the central engine activity duration, named ‘tip-of-iceberg’ effect (Lü et al. 2014; Zhang et al. 2014; Li et al. 2016; Gao et al. 2017a; Liu et al. 2017c). A longer accretion timescale need to explain these observations by the BH hyperaccretion systems. The durations of the compact binary mergers are not necessarily to be “short”, and in principle the collapsar model can also bring forth SGRBs (e.g., Janiuk & Proga 2008; Zhang et al. 2009). If it is the case, the values of the jet luminosities and timescales of GRBs are larger than these in Table 1. Thus the applicability of our model will face the greater challenges than in the current situations.

Table 1. GRBs data

| Name | T_{90} | z | $E_{\gamma,\text{iso}}$ | $E_{\text{k,iso}}$ | $E_{\text{p,rest}}$ | θ_j | L_j | Ref |
|-------|----------|-----|-------------------------|--------------------|---------------------|------------|-------------------------|-----|
| | (s) | | (10^{52} erg) | (10^{52} erg) | (keV) | (rad) | (erg s^{-1}) | |
| (1) | (2) | (3) | (4) | (5) | (6) | (7) | (8) | (9) |
| SGRBs | | | | | | | | |

Table 1 continued

Table 1 (*continued*)

| Name | T_{90} | z | $E_{\gamma, \text{iso}}$ | $E_{k, \text{iso}}$ | $E_{p, \text{rest}}$ | θ_j | L_j | Ref |
|--------------|-------------------|--------|--------------------------------|-------------------------------|---------------------------------|------------------------------|-------------------------|----------|
| (1) | (s) | (3) | (10^{52} erg) | (10^{52} erg) | (keV) | (rad) | (erg s^{-1}) | (9) |
| 050509B | 0.04 | 0.225 | $0.00024^{+0.00044}_{-0.0001}$ | 0.0055 | $100.45^{+748.475}_{-98}$ | > 0.05 | 0.022 | 1, 2 |
| 050709 | 0.07 | 0.161 | 0.0027 ± 0.0011 | 0.0016 | $96.363^{+20.898}_{-13.932}$ | > 0.26 | 0.2397 | 1, 3 |
| 050724A | 3 | 0.257 | $0.009^{+0.011}_{-0.002}$ | 0.027 | $138.27^{+502.8}_{-56.565}$ | > 0.35 | 0.0915 | 1, 2 |
| 051210 | 1.3 | 1.3 | $0.4^{+0.5}_{-0.2}$ | 0.238 | 943^{+1495}_{-598} | > 0.05 | 0.1411 | 1, 2 |
| 051221A | 1.4 | 0.5465 | $0.28^{+0.21}_{-0.1}$ | 1.26 | $603.135^{+1020.69}_{-293.835}$ | 0.12 | 1.2234 | 1, 2 |
| 060502B | 0.09 | 0.287 | $0.003^{+0.005}_{-0.002}$ | 0.012 | $437.58^{+926.64}_{-244.53}$ | > 0.05 | 0.0268 | 1, 2 |
| 060801 | 0.5 | 1.13 | $0.7^{+1.5}_{-0.5}$ | 0.071 | $1320.6^{+2279.1}_{-724.2}$ | $0.0561^{+0.0056}_{-0.0063}$ | 0.5167 | 1, 2, 4 |
| 061006 | 0.4 | 0.438 | 3^{+4}_{-1} | 0.314 | $819.66^{+1308.58}_{-402.64}$ | $0.407^{+0.068}_{-0.173}$ | 97.3211 | 1, 2, 4 |
| 061201 | 0.8 | 0.111 | 3^{+4}_{-2} | 0.007 | $666.6^{+888.8}_{-388.85}$ | 0.017 | 0.0603 | 1, 2 |
| 061210 | 0.2 | 0.409 | $0.09^{+0.16}_{-0.05}$ | 0.086 | $760.86^{+1070.84}_{-436.79}$ | > 0.37 | 8.3909 | 1, 2, 5 |
| 070429B | 0.5 | 0.902 | $0.07^{+0.11}_{-0.02}$ | 0.451 | $228.24^{+1418.89}_{-125.532}$ | > 0.05 | 0.2477 | 1, 2 |
| 070714B | 2.0 | 0.923 | $1.16^{+0.41}_{-0.22}$ | 0.232 | $2153.76^{+1499.94}_{-730.74}$ | $0.33^{+0.11}_{-0.11}$ | 7.2217 | 1, 3, 4 |
| 070724A | 0.4 | 0.457 | 0.003 ± 0.001 | 0.099 | 99 | $0.27^{+0.16}_{-0.16}$ | 1.346 | 1, 3, 4 |
| 070729 | 0.9 | 0.8 | 0.017 | 0.132 | 840.6^{+1526}_{-351} | > 0.05 | 0.0372 | 1, 6 |
| 070809 | 1.3 | 0.473 | 0.0056 | 0.391 | $75.6^{+12.6}_{-13.9}$ | $0.4^{+0.08}_{-0.333}$ | 3.5473 | 1, 4, 6 |
| 071227 | 1.8 | 0.381 | 0.1 ± 0.02 | 0.025 | 1384 ± 277 | > 0.0262 | 0.0033 | 1, 5, 7 |
| 080905A | 1.0 | 0.122 | 0.0005 | 0.0024 | $502.8^{+950.6}_{-280.5}$ | $0.28^{+0.15}_{-0.16}$ | 0.0127 | 1, 4, 6 |
| 090426* | 1.2 | 2.609 | 0.5 ± 0.1 | 13.5 | 177^{+90}_{-65} | 0.07 | 10.3115 | 1, 8 |
| 090510 | 0.3 | 0.903 | $4.47^{+4.06}_{-3.77}$ | 0.307 | $7490^{+532.8}_{-494.8}$ | 0.017 | 0.4379 | 1, 6 |
| 090515 | 0.04 | 0.403 | 0.0008 | 0.062 | $90.1^{+47.4}_{-16.8}$ | > 0.05 | 0.2753 | 1, 6 |
| 100117A | 0.3 | 0.92 | 0.09 ± 0.01 | 0.11 | 551^{+142}_{-96} | $0.27^{+0.15}_{-0.15}$ | 4.6373 | 1, 4, 7 |
| 100206A | 0.1 | 0.408 | $0.0763^{+0.0789}_{-0.0229}$ | 0.0073 | $638.98^{+131.21}_{-131.21}$ | > 0.05 | 0.1471 | 1, 9 |
| 100625A | 0.3 | 0.453 | 0.075 ± 0.003 | 0.0093 | 701.32 ± 114.71 | > 0.05 | 0.051 | 1, 10 |
| 101219A | 0.6 | 0.718 | 0.49 ± 0.07 | 0.045 | 842^{+177}_{-136} | $0.29^{+0.14}_{-0.14}$ | 6.3966 | 1, 4, 7 |
| 111117A | 0.5 | 1.3 | 0.338 ± 0.106 | 0.377 | 966 ± 322 | 0.105 | 1.8114 | 1, 10 |
| 120804A | 0.81 | 1.3 | 0.7 | 0.7 | $310.5^{+151.8}_{-66.7}$ | > 0.19 | 7.1539 | 11 |
| 130603B | 0.18 | 0.356 | 0.212 ± 0.023 | 0.28 | 900 ± 140 | 0.07 | 0.9077 | 1, 10 |
| 131001A | 1.54 | 0.717 | 0.037 | 0.541 | 94.44 ± 24.04 | > 0.05 | 0.0805 | 1, 12 |
| 140622A | 0.13 | 0.959 | 0.0065 | 0.977 | 86.2 ± 15.67 | > 0.05 | 1.8522 | 1, 13 |
| 160821B | 0.48 | 0.16 | 0.021 ± 0.002 | 8 | 97.44 ± 22.04 | 0.063 | 3.8455 | 14, 15 |
| LGRBs | | | | | | | | |
| 970508 | 14.0 ± 3.6 | 0.8349 | 0.61 ± 0.13 | 0.99 ± 0.14 | 145 ± 43 | 0.3775 ± 0.0291 | 1.4765 | 16, 17 |
| 970828 | 160.0 | 0.96 | 29 ± 3 | 37.154 | 586 ± 117 | 0.1239 | 0.6212 | 16, 18 |
| 971214 | 31.23 ± 1.18 | 3.418 | 21 ± 3 | 8.48 ± 0.97 | 685 ± 133 | $> 0.0967 \pm 0.0040$ | 1.9483 | 16, 17 |
| 980613 | 42.0 ± 22.1 | 1.0964 | 0.59 ± 0.09 | 1.22 ± 0.38 | 194 ± 89 | $> 0.2194 \pm 0.0101$ | 0.2166 | 16, 17 |
| 980703 | 76.0 ± 10.2 | 0.966 | 7.2 ± 0.7 | 2.41 ± 0.63 | 503 ± 64 | 0.1957 ± 0.0141 | 0.4745 | 16, 17 |
| 990123 | 63.3 ± 0.3 | 1.61 | 229 ± 37 | 534 | 1724 ± 446 | 0.064 ± 0.005 | 6.4408 | 16, 19 |
| 990510 | 67.58 ± 1.86 | 1.619 | 17 ± 3 | 13.16 ± 1.12 | 423 ± 42 | 0.0586 ± 0.0037 | 0.2006 | 16, 17 |
| 990705 | 32.0 ± 1.4 | 0.84 | 18 ± 3 | 0.34 ± 0.12 | 459 ± 139 | 0.0930 ± 0.0072 | 0.4557 | 16, 17 |
| 991216 | 15.17 ± 0.091 | 1.02 | 67 ± 7 | 36.64 ± 1.79 | 648 ± 134 | 0.0798 ± 0.0126 | 4.3918 | 16, 17 |
| 000210 | 9.0 ± 1.4 | 0.846 | 14.9 ± 1.6 | 0.50 ± 0.12 | 753 ± 26 | $> 0.1194 \pm 0.0049$ | 2.2489 | 16, 17 |
| 000926 | 1.30 ± 0.59 | 2.0387 | 27.1 ± 5.9 | 9.97 ± 3.75 | 310 ± 20 | 0.1075 ± 0.0054 | 50.0191 | 16, 17 |
| 010222 | 74.0 ± 4.1 | 1.4769 | 81 ± 9 | 22.79 ± 2.48 | 766 ± 30 | 0.0559 ± 0.0023 | 0.5426 | 16, 17 |
| 011211 | 51.0 ± 7.6 | 2.14 | 5.4 ± 0.6 | 71.32 ± 0.22 | 186 ± 24 | 0.1114 ± 0.0070 | 2.9279 | 16, 17 |
| 020813 | 89 | 1.25 | 66 ± 16 | 204.174 | 590 ± 151 | 0.0541 | 0.9993 | 16, 18 |
| 021004 | 77.1 ± 2.6 | 2.3304 | 3.3 ± 0.4 | 8.35 ± 1.45 | 266 ± 117 | 0.2211 ± 0.0787 | 1.225 | 16, 17 |
| 050126 | 30 | 1.29 | $0.8^{+1.0}_{-0.2}$ | 39.8 ± 80.4 | $387.01^{+1135.84}_{-144.27}$ | $0.365^{+0.095}_{-0.125}$ | 20.4159 | 2, 4, 20 |
| 050315 | 96 ± 10 | 1.9500 | $5.7^{+6.2}_{-0.1}$ | $512.403^{+45.299}_{-65.577}$ | $126.85^{+32.45}_{-123.9}$ | $0.0759^{+0.0080}_{-0.0091}$ | 4.5837 | 2, 17 |

Table 1 (*continued*)

Table 1 (*continued*)

| Name | T_{90} | z | $E_{\gamma, \text{iso}}$ | $E_{k, \text{iso}}$ | $E_{p, \text{rest}}$ | θ_j | L_j | Ref |
|---------|------------------|--------|-------------------------------|--------------------------------|---------------------------------|------------------------------|-------------------------|-----------|
| (1) | (s) | (3) | (10^{52} erg) | (10^{52} erg) | (keV) | (rad) | (erg s^{-1}) | (9) |
| 050318 | 32 ± 2 | 1.4436 | 2.2 ± 0.16 | $11.259^{+0.867}_{-0.685}$ | 115 ± 25 | 0.0380 ± 0.0070 | 0.0742 | 16, 17 |
| 050319 | 139.4 ± 8.2 | 3.2425 | $4.6^{+6.5}_{-0.6}$ | $77.896^{+20.496}_{-28.695}$ | $190.912^{+114.548}_{-182.428}$ | $0.0380^{+0.0051}_{-0.0070}$ | 0.1812 | 2, 17 |
| 050401 | 38 | 2.9 | 35 ± 7 | 4570.9 ± 1317.6 | 467 ± 110 | $0.472^{+0.02}_{-0.044}$ | 5168.5851 | 4, 16, 20 |
| 050416A | 5.4 | 0.654 | 0.1 ± 0.01 | 15.1 ± 3.9 | 25.1 ± 4.2 | $0.237^{+0.114}_{-0.059}$ | 13.0142 | 4, 16, 20 |
| 050505 | 63 ± 2 | 4.27 | 16^{+13}_{-3} | $237.829^{+98.405}_{-49.203}$ | $737.8^{+1807.61}_{-226.61}$ | $0.0290^{+0.0059}_{-0.0030}$ | 0.8928 | 2, 17 |
| 050525 | 11.5 | 0.606 | 2.5 ± 0.43 | 28.2 ± 8.1 | 127 ± 10 | $0.0551^{+0.0069}_{-0.0062}$ | 0.6507 | 4, 16, 20 |
| 050730 | 155 ± 20 | 3.97 | 9^{+8}_{-3} | 86.1223 | $974.12^{+2798.11}_{-432.39}$ | > 0.023 | 0.0807 | 2, 19 |
| 050802 | 20 | 1.71 | $1.8197^{+1.6477}_{-0.30614}$ | 616.6 ± 295.4 | $268.3^{+623.3}_{-75.9}$ | $0.29^{+0.15}_{-0.15}$ | 349.8991 | 4, 20, 21 |
| 050814 | 48 | 5.3 | 6^{+3}_{-1} | 831.764 | $403.2^{+378}_{-138.6}$ | 0.0419 | 9.6506 | 2, 18 |
| 050820A | 600 | 2.615 | 97.4 ± 7.8 | 53.7145 | 1325 ± 277 | 0.184 | 1.5369 | 16, 19 |
| 050904 | 183.6 ± 13.2 | 6.295 | 124 ± 13 | $88.37^{+86.3}_{-44.2}$ | 3178 ± 1094 | 0.0340 ± 0.0051 | 0.4877 | 16, 17 |
| 050922C | 4.5 | 2.198 | 5.3 ± 1.7 | 47.725 | 415 ± 111 | 0.026 | 1.2736 | 16, 19 |
| 051109A | 360 | 2.35 | 6.5 ± 0.7 | 169.824 | 539 ± 200 | 0.0593 | 0.2884 | 16, 18 |
| 060124 | 298 ± 2 | 2.297 | 41 ± 6 | $578.87^{+110.79}_{-12.66}$ | 784 ± 285 | $0.0531^{+0.0091}_{-0.0040}$ | 0.9666 | 16, 17 |
| 060206 | 5.0 ± 0.7 | 4.05 | 4.3 ± 0.9 | 386.76 ± 93.02 | 394 ± 46 | 0.0351 ± 0.0010 | 24.3279 | 16, 17 |
| 060210 | 220 ± 70 | 3.91 | 42^{+35}_{-8} | 1313.2261 | $667.76^{+1703.77}_{-191.49}$ | 0.024 ± 0.002 | 0.871 | 2, 19 |
| 060418 | 52 ± 1 | 1.49 | 13 ± 3 | 7.5307 | 572 ± 143 | 0.029 ± 0.006 | 0.0413 | 16, 19 |
| 060505* | 4 ± 1 | 0.089 | 0.0012 ± 0.0002 | 0.028 | $482.4^{+524.8}_{-167.7}$ | ~ 0.4 | 0.06275 | 6, 22, 23 |
| 060526 | 258.8 ± 5.4 | 3.21 | 2.6 ± 0.3 | $15.58^{+0.24}_{-0.21}$ | 105 ± 21 | 0.0630 ± 0.0010 | 0.0587 | 16, 17 |
| 060605 | 19 ± 1 | 3.8 | $2.5^{+3.1}_{-0.6}$ | 115 | $681.6^{+1723.2}_{-240}$ | > 0.046 | 3.14 | 2, 19 |
| 060607A | 100 ± 5 | 3.082 | 9^{+7}_{-2} | 0.822 | $567.398^{+889.876}_{-167.362}$ | > 0.095 | 0.1808 | 2, 19 |
| 060614* | 6.9 | 0.12 | 0.21 ± 0.09 | 1.698 | 55 ± 45 | 0.2025 | 0.6328 | 16, 18 |
| 060707 | 210.0 | 3.42 | 5.4 ± 1 | 102.329 | 279 ± 28 | 0.1379 | 2.1525 | 16, 18 |
| 060714 | 108.2 ± 6.4 | 2.71 | $7.7^{+7.5}_{-0.9}$ | 250.46 ± 248.11 | $196.63^{+348.74}_{-181.79}$ | 0.0201 ± 0.0010 | 0.1788 | 2, 17 |
| 060908 | 18.0 ± 0.8 | 1.8836 | 9.8 ± 0.9 | $2017.68^{+2522.09}_{-504.42}$ | 514 ± 102 | $0.0080^{+0.0051}_{-0.0010}$ | 1.0394 | 16, 17 |
| 061007 | 75 ± 5 | 1.262 | 86 ± 9 | 29.9425 | 890 ± 124 | > 0.138 | 3.3244 | 16, 19 |
| 061021 | 79.0 | 0.35 | 10^{+8}_{-4} | 6.166 | $661.5^{+985.5}_{-337.5}$ | 0.1501 | 0.3106 | 2, 18 |
| 061121 | 81 ± 5 | 1.314 | 22.5 ± 2.6 | 20.5215 | 1289 ± 153 | 0.099 | 0.6018 | 16, 19 |
| 061222A | 16.0 | 2.09 | 21^{+11}_{-4} | 2290.868 | $710.7^{+747.78}_{-210.12}$ | 0.0471 | 49.5146 | 2, 18 |
| 070110 | 89 ± 7 | 2.352 | $3.0^{+2.5}_{-0.5}$ | 0.687 | $372.072^{+1035.77}_{-90.504}$ | > 0.274 | 0.518 | 2, 19 |
| 070125 | 63.0 ± 1.7 | 1.5477 | 80.2 ± 8 | $6.43^{+0.9}_{-0.17}$ | 934 ± 148 | 0.2304 ± 0.0105 | 9.2574 | 16, 17 |
| 070306 | 3.0 | 1.5 | 6^{+5}_{-1} | 67.608 | $300^{+1340}_{-97.5}$ | 0.0768 | 18.081 | 2, 18 |
| 070318 | 63 ± 3 | 0.84 | $0.9^{+0.9}_{-0.2}$ | 47.2719 | $360.64^{+818.8}_{-143.52}$ | 0.127 ± 0.008 | 1.1331 | 2, 19 |
| 070411 | 101 ± 5 | 2.95 | 10^{+8}_{-2} | 83.6596 | $474^{+2196.2}_{-154.05}$ | 0.032 ± 0.005 | 0.1875 | 2, 19 |
| 070508 | 23.4 | 0.82 | 8^{+2}_{-1} | 10.715 | $378.56^{+138.32}_{-74.62}$ | 0.0611 | 0.2716 | 2, 18 |
| 071010A | 6 ± 1 | 0.98 | 0.13 ± 0.01 | 7.2164 | $73^{+97.7}_{-69.9}$ | 0.090 ± 0.008 | 0.9812 | 19, 21 |
| 071010B | 35.7 ± 0.5 | 0.947 | 1.7 ± 0.9 | 7.2713 | 101 ± 20 | 0.150 ± 0.006 | 0.5494 | 16, 19 |
| 071031 | 150.5 | 2.692 | 3.9 ± 0.6 | 1.554 | $45.23^{+22.85}_{-41.54}$ | 0.070 ± 0.013 | 0.0328 | 19, 21 |
| 080310 | 32.0 | 2.43 | 6.0256 | 29.512 | $75.4^{+72}_{-30.8}$ | 0.0628 | 0.7509 | 18, 21 |
| 080319C | 29.55 | 1.95 | 14.1 ± 2.8 | 74.4078 | 906 ± 272 | > 0.102 | 4.5924 | 16, 19 |
| 080330 | 61 ± 9 | 1.51 | 0.21 ± 0.05 | 21.0923 | < 88 | > 0.087 | 0.3315 | 19, 24 |
| 080413B | 8.0 | 1.1 | 2.4 ± 0.3 | 138.038 | 150 ± 30 | 0.1047 | 20.1874 | 18, 25 |
| 080603A | 150 | 1.688 | 2.2 ± 0.8 | 52.5129 | 160^{+920}_{-130} | 0.071 ± 0.011 | 0.247 | 19, 26 |
| 080710 | 120 ± 17 | 0.845 | 0.8 ± 0.4 | 2.6451 | 200 | > 0.062 | 0.0102 | 19, 27 |
| 080810 | 108 ± 5 | 3.35 | 45 ± 5 | 41.8519 | 1470 ± 180 | > 0.105 | 1.9266 | 19, 25 |
| 080913* | 8 ± 1 | 6.695 | 8.6 ± 2.5 | ≤ 10 | 710 ± 350 | $0.359^{+0.125}_{-0.099}$ | 114.0568 | 4, 25 |
| 081008 | 162.2 ± 25.0 | 1.967 | $9.98^{+2.34}_{-2.31}$ | $134.7^{+18.3}_{-17.3}$ | 255.9 ± 57.47 | 0.0227 ± 0.0070 | 0.0682 | 17, 28 |
| 081203A | 223 | 2.1 | 35 ± 3 | 11.2261 | 1541 ± 757 | > 0.116 | 0.4319 | 19, 29 |

Table 1 *continued*

Table 1 (*continued*)

| Name | T_{90} | z | $E_{\gamma, \text{iso}}$ | $E_{k, \text{iso}}$ | $E_{p, \text{rest}}$ | θ_j | L_j | Ref |
|---------|--------------------|--------|--------------------------|---------------------|--------------------------------|------------------------------|-------------------------|--------|
| | (s) | | (10^{52} erg) | (10^{52} erg) | (keV) | (rad) | (erg s^{-1}) | |
| (1) | (2) | (3) | (4) | (5) | (6) | (7) | (8) | (9) |
| 081222 | 5.8 | 2.77 | 30 ± 3 | 131.826 | 505 ± 34 | 0.0489 | 12.5737 | 18, 25 |
| 090313 | 78 ± 19 | 3.375 | 3.2 | 276.8523 | $240.1_{-223.5}^{+885.4}$ | > 0.093 | 6.7881 | 19, 21 |
| 090323 | 133.1 ± 1.4 | 3.568 | 410 ± 50 | 116_{-9}^{+13} | 1901 ± 343 | $0.0489_{-0.0017}^{+0.0070}$ | 2.1579 | 17, 25 |
| 090328 | 57 ± 3 | 0.7354 | 13 ± 3 | 82_{-18}^{+28} | 1028 ± 312 | $0.0733_{-0.0140}^{+0.0227}$ | 0.7767 | 17, 25 |
| 090423* | 10.3 ± 1.1 | 8.23 | 11 ± 3 | 340_{-140}^{+110} | 491 ± 200 | $0.0262_{-0.0052}^{+0.0122}$ | 10.7949 | 17, 25 |
| 090424 | 49.47 ± 0.9 | 0.544 | 4.6 ± 0.9 | 53.1215 | 273 ± 50 | > 0.378 | 12.718 | 19, 25 |
| 090812 | 75.9 | 2.452 | 40.3 ± 4 | 148.827 | 2023 ± 663 | > 0.071 | 2.1671 | 19, 29 |
| 090902B | 19.328 ± 0.286 | 1.8829 | 1.77 ± 0.01 | 56_{-7}^{+3} | 596.76 ± 17.2974 | 0.0681 ± 0.0035 | 1.9973 | 3, 17 |
| 090926A | 20 ± 2 | 2.1062 | 210_{-8}^{+9} | 6.8 ± 0.2 | 1279.75 ± 62.124 | $0.1571_{-0.0349}^{+0.0698}$ | 41.4656 | 3, 17 |
| 091018 | 106.5 | 0.97 | 0.5888 | 12.023 | 51.29 ± 23.7 | 0.0820 | 0.0784 | 18, 28 |
| 091020 | 65 | 1.71 | 12.2 ± 2.4 | 51.286 | 129.809 ± 19.241 | 0.1204 | 1.9162 | 7, 18 |
| 091024 | 1020 | 1.092 | 28 ± 3 | 37.2529 | 794 ± 231 | > 0.071 | 0.0337 | 19, 29 |
| 091029 | 39.2 | 2.752 | 7.4 ± 0.74 | 40.303 | 230 ± 66 | > 0.192 | 8.39 | 19, 29 |
| 091208B | 71 | 1.063 | 2.01 ± 0.07 | 50.119 | $297.4846_{-28.6757}^{+37.13}$ | 0.1274 | 1.2276 | 7, 18 |
| 100418A | 8.0 ± 2.0 | 0.6235 | $0.99_{-0.34}^{+0.63}$ | 3.36 | $47.08_{-43.83}^{+3.247}$ | 0.3560 | 5.5352 | 30, 31 |
| 100621A | 63.6 ± 1.7 | 0.542 | 4.37 ± 0.5 | 111.7596 | 146 ± 23.1 | > 0.234 | 7.6734 | 19, 29 |
| 100728B | 12.1 ± 2.4 | 2.106 | 2.66 ± 0.11 | 95.665 | 406.886 ± 46.59 | > 0.063 | 5.0071 | 7, 19 |
| 100901A | 439 | 1.408 | 6.3 | 167.3233 | 230 | 0.152 | 1.098 | 19, 32 |
| 100906A | 114.4 ± 1.6 | 1.727 | 28.9 ± 0.3 | 23.8173 | $289.062_{-55.0854}^{+47.72}$ | 0.055 ± 0.002 | 0.19 | 7, 19 |
| 110205A | 257 ± 25 | 2.22 | 56 ± 6 | 31.2172 | 715 ± 239 | 0.064 | 0.2237 | 19, 29 |
| 110213A | 48 ± 6 | 1.46 | 6.9 ± 0.2 | 25.7527 | $242.064_{-16.974}^{+20.91}$ | > 0.142 | 1.6843 | 7, 19 |
| 120119A | 70 ± 4 | 1.728 | 36 | 4.17 | 498.9 ± 22.31 | 0.032 ± 0.002 | 0.0801 | 19, 28 |
| 120326A | 11.8 ± 1.8 | 1.798 | 3.2 ± 0.1 | 14.0 ± 0.07 | 152 \pm 14 | 0.0803 ± 0.0035 | 1.3142 | 17, 33 |
| 120521C | 26.7 ± 0.4 | 6 | $8.25_{-1.96}^{+2.24}$ | 22_{-14}^{+37} | 682_{-207}^{+845} | $0.0524_{-0.0192}^{+0.0401}$ | 1.0885 | 17, 34 |

* GRBs have unusual characteristics on observations (Xin et al. 2011; Zhang et al. 2009).

References:

(1) Liu et al. (2015a); (2) Butler et al. (2007); (3) Zhang (2011); (4) Ryan et al. (2015); (5) Racusin et al. (2009); (6) Kann et al. (2011); (7) Zhang et al. (2012); (8) Antonelli et al. (2009); (9) Tsutsui et al. (2013); (10) Zaninoni et al. (2016); (11) Berger et al. (2013b); (12) Cummings et al. (2013); (13) Sakamoto et al. (2014); (14) Stanbro & Meegan (2016); (15) Lü et al. (2017); (16) Amati et al. (2008); (17) Song et al. (2016); (18) Nemmen et al. (2012); (19) Yi et al. (2016); (20) Zhang et al. (2007b); (21) Kann et al. (2010); (22) Xu et al. (2009); (23) Ofek et al. (2007); (24) Guidorzi et al. (2009); (25) Amati et al. (2009); (26) Guidorzi et al. (2011); (27) Krühler et al. (2009); (28) Dichiara et al. (2016); (29) Ghirlanda et al. (2012); (30) Marshall et al. (2011); (31) Laskar et al. (2015); (32) Gorbovskoy et al. (2012); (33) Demianski et al. (2017); (34) Yasuda et al. (2017).

4. QUASI-SNE

As strong GW sources in the nearby galaxies, the NS-NS/BH-NS mergers are expected to have electromagnetic counterparts such as SGRBs (e.g., Eichler et al. 1989; Nakar 2007; Berger 2014; Kumar & Zhang 2015; Levan et al. 2016), off-axis emission of SGRB jets (e.g., Rhoads 1999; Lazzati et al. 2017; Xiao et al. 2017), optical/NIR signals powered by the decay of heavy radioactive elements in the ejection matter (e.g., Li & Paczyński 1998; Metzger 2017), radio flares (e.g., Nakar & Piran 2011; Gao et al. 2013; Piran et al. 2013), or X-ray emission from GRB central engine (e.g., Nakamura et al. 2014; Kisaka et al. 2015). Furthermore, Zhang (2013) proposed that potentially an early X-ray afterglow would continue for thousands of seconds

followed GW bursts once the NS-NS merger produced a magnetar rather than a BH. The existence of X-ray transient is likely a difference between the magnetar and the BH hyperaccretion from observations (Sun et al. 2017).

As mentioned above, the compact objects merger model is possibly accompanied by the ejection of neutron-rich matter. The dynamical ejecta, in a typical timescale of milliseconds, constitute contact-interface materials which are squeezed out by the hydrodynamic force (e.g., Oechslin et al. 2007; Bauswein et al. 2013; Hotokezaka et al. 2013) or the tidal force (e.g., Kawaguchi et al. 2015). For NS-NS mergers, the typical ejecta velocity and mass are in the range of $\sim 0.1 - 0.3 c$ and $\sim 10^{-4} - 10^{-2} M_{\odot}$, respectively (e.g., Hotokezaka et al. 2013). Recent BH-NS merger

simulations revealed that the ejecta mass could reach $0.1 M_{\odot}$ with a similar velocity as in the NS-NS cases (Kawaguchi et al. 2015, 2016). Then heavy radioactive elements will form via the r-process of neutron-rich matter. The radioactive decay of these elements provides a source for powering transient optical/NIR emission (Eichler et al. 1989; Li & Paczyński 1998), named ‘kilonova’ (Kulkarni 2005) [also called ‘macronova’ (Metzger et al. 2010)].

In addition to the radioactivity of the merger ejecta, the remnant materials’ fall-back accretion (e.g., Rosswog 2007; Rossi & Begelman 2009; Chawla et al. 2010; Kyutoku et al. 2015), the ejecta from the disk, like winds (e.g., Metzger & Berger 2012; Ma et al. 2017) or outflows, and magnetars (e.g., Zhang 2013; Gao et al. 2013; Yu et al. 2013; Metzger & Piro 2014; Gao et al. 2015, 2017b) can also power kilonovae. For some SGRBs with extended emission or internal X-ray plateaus, the magnetars might form after NS-NS mergers and provide the additional energy injection into the ejecta to power ‘mergernovae’ (e.g., Yu et al. 2013).

The kilonovae are claimed to be detected in the optical/NIR band, associated with some GRBs, i.e., GRBs 050709 (Jin et al. 2016), 060614 (Yang et al. 2015; Jin et al. 2015; Horesh et al. 2016), 130603B (Tanvir et al. 2013; Berger et al. 2013a; Fan et al. 2013), and 160821B (Kasliwal et al. 2017). The excess optical emission was also discovered in GRB 080503 with a lack of redshift (Perley et al. 2009). Gao et al. (2017b) revisited the *Swift* SGRB samples and found three ‘magnetar-powered mergernova’ candidates, i.e., GRBs 050724, 070714B, and 061006. The luminosities of these sources are ten times or a hundred times higher than those of typical kilonovae. For the recent GW event, the luminosity of GRB 170817A is one order of magnitude lower than that of associated AT 2017gfo (e.g., Smartt et al. 2017).

Considering the existence of abundant outflow materials, the luminosity of kilonovae may be much higher. Following Li & Paczyński (1998), we adopt a power law decay model here, and assume the material envelope expanding uniformly with the fixed velocity V , constant mass M , surface radius R , and density ρ . The critical time t_c , when the optical depth of the expanding sphere satisfies $\kappa\rho R = 1$, can be calculated as

$$t_c = \left(\frac{3\kappa M}{4\pi V^2}\right)^{1/2} \\ = 1.13 \text{ day} \left(\frac{M}{0.01 M_{\odot}}\right)^{1/2} \left(\frac{3V}{c}\right)^{-1} \left(\frac{\kappa}{\kappa_e}\right)^{1/2}, \quad (5)$$

where $\kappa \sim \kappa_e$ and $\kappa_e \sim 0.1 \text{ cm}^2 \text{ g}^{-1}$ (e.g., Metzger et al. 2010) represent the average opacity and the electron scattering, respectively, and $V = 0.1 c$ is adopted. The luminosity of a kilonova powered by the radioactive de-

cah of nuclei can be estimated as

$$L_{\text{kilo}} = L_0 \sqrt{\frac{8\beta}{3}} Y \left(\sqrt{\frac{3}{8\beta}} \tau \right), \quad (6)$$

where $L_0 = 3\eta M c^2 / (4\beta t_c)$, $\tau = t/t_c$, and $\beta = V/c$. $\eta = 3 \times 10^{-6}$ denotes the fraction of rest-mass energy released in radioactive decay (Metzger et al. 2010), and $Y(x) = e^{-x^2} \int_0^x e^{k^2} dk$ is the Dawson’s integral.

By assuming blackbody emission, the effective temperature of the thermal emission is given by

$$T_{\text{eff}} = \left(\frac{L_{\text{kilo}}}{4\pi\sigma R_{\text{ph}}^2} \right)^{1/4}, \quad (7)$$

where σ is the Stephan-Boltzmann constant, and R_{ph} is the photosphere radius corresponding the radius of mass shell when the optical depth is equal to 1.

The flux density of the source at photon frequency ν can be described as follows,

$$F_{\nu} = \frac{2\pi h\nu^3}{c^2} \frac{1}{e^{h\nu/kT_{\text{eff}}} - 1} \frac{R_{\text{ph}}^2}{D^2}. \quad (8)$$

Then we can get the luminosity of an observational frequency ν , i.e.,

$$\nu L_{\nu} = \nu 4\pi D^2 F_{\nu} = \frac{8\pi^2 h\nu^4 R_{\text{ph}}^2}{c^2} \frac{1}{e^{h\nu/kT_{\text{eff}}} - 1}. \quad (9)$$

The total luminosities of kilonovae are shown in Figure 2(a). Lines in different color (black, red, blue, green, magenta) correspond to different values of λ , m_{re} , and f . Thick solid parts and thin dotted parts indicate the expanding spheres in the optically-thick and optically-thin, respectively. We notice that the luminosities of kilonovae increase with the increase of the outflow ratios and residual masses.

Figure 2(b) displays the optical ($\sim 1 \text{ eV}$) light curves of kilonovae, in comparison with SNe and mergernovae. The gray filled stars and circles respectively represent the data of SN 2013dx and SN 1994I. The grey solid and dashed lines depict the optical light curves of the millisecond-magnetar-powered mergernovae, which are adapted from Figure 3 in Yu et al. (2013).

From Figure 1 and Figure 2, one can conclude that the energies of a GRB and its associated kilonova appear to be complementary to each other, mainly depending on the neutron-rich outflow ratio. Comparing those light curves, we find that for strong outflows and massive remnants, the durations of the kilonovae powered by the outflows are much longer than those of mergernovae, even approaching those of SNe. That is, the more massive accretion materials become the outflows, the more similar the behaviors of kilonovae become faint SNe, especially the SNe with the steep decay such as SN 2002bj and SN 2010X. Therefore, we prefer the name ‘quasi-SNe’ for these phenomena, and we expect that a

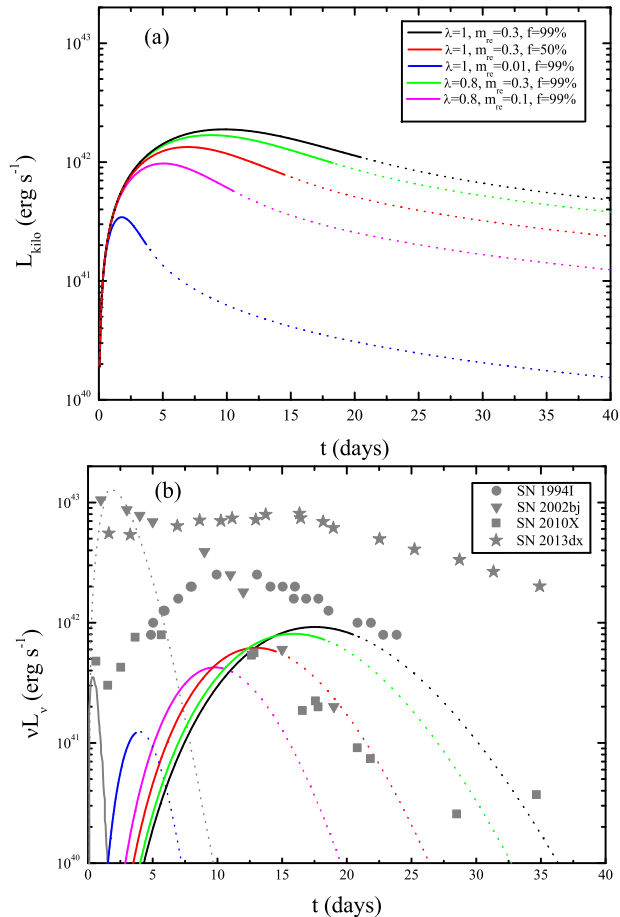


Figure 2. (a) Total luminosity of kilonovae. (b) Comparisons of the optical (~ 1 eV) light curves with SNe and mergernovae. Lines in different colors (black, red, blue, green, magenta) correspond to different values of λ , m_{re} , and f . Thick solid parts and thin dotted parts indicate the expanding spheres in the optically-thick and optically-thin, respectively. The gray filled circles, triangles, squares, and stars represent SN 1994I, SN 2002bj, SN 2010X, and SN 2013dx data, respectively. The grey solid and dashed lines depict optical light curves of the millisecond-magnetar-powered mergernovae.

new type of ‘nova’ like the faint SNe may be detected after merger events. In addition, the vertical distribution of the outflows might effect the luminosity of the kilonovae for different view angles.

5. SUMMARY

The progenitors of GRBs remain mysteries after about fifty years’ discussions. It is still difficult to identify the physical origin of a GRB with multi-wavelength observational data available. The traditional definition of SGRBs and LGRBs by T_{90} might not shed light on their progenitors.

After the mergers of NS-NS or BH-NS, a BH might be born surrounded by a hyperaccretion disk. In

the present work, we test the applicability of the BH hyperaccretion inflow-outflow model on powering both LGRBs and SGRBs in the compact binary merger scenario. If about half of the disk materials become outflows, the luminosity and duration of the hyperaccretion processes might satisfy the requirements of not only all SGRBs but also account for most of LGRBs. We also point out that, to verify the origin of GRBs one may need various information, including the characteristics of host galaxies, the SN associations, and the spectral lags, etc.

The optical/NIR emission observed in GRB afterglows are possibly powered by the numerous energy sources (for reviews, see e.g., Metzger 2017). Here we propose a new mechanism of a BH hyperaccretion disk with extreme strong neutron-rich outflows, named quasi-SNe. The luminosities and timescales of quasi-SNe depend significantly on the outflow strengths. Consequently, there is a severe competition between GRBs and the associated quasi-SNe on the disk mass and energy budgets. In contrast, the luminosity of a mergernova depend on the energy injection from a magnetar, and there is no obvious correlation between it and the GRB luminosity, since most of the spin-down energy would be dissipated via GW emission (e.g., Liu et al. 2017b). In the particular case of GRB 170817A and AT2017gfo, our model can naturally explain a weak GRB associated by a bright kilonova by considering the vertical distribution of the outflows, even without an off-axis jet for observers (e.g., Lazzati et al. 2017; Xiao et al. 2017; Zhang et al. 2017). We will investigate further this point in our future work.

Very possibly in the near future, more and more GWs’ electromagnetic counterparts could be confirmed, produced by the compact binary mergers (especially for NS-NS and NS-BH). Noted that their optical/NIR emission might be originated from three mechanism: the ejecta or winds (kilonovae), the injection energy of magnetars (mergernovae), or the strong outflows from the hyperaccretion disks (quasi-SNe).

A Note Added. This paper was posted in arXiv at Sept. 30th, 2017. The discussion on GW 170817/GRB 170817A/AT2017gfo was added in the revised version after addressing referee’s comments.

We thank Zi-Gao Dai, Bing Zhang, and Tuan Yi for helpful comments and discussions. This work was supported by the National Basic Research Program of China (973 Program) under grant 2014CB845800 and the National Natural Science Foundation of China under grants 11473022 and U1431107.

REFERENCES

- Abadie, J., Abbott, B. P., Abbott, R., et al. 2010, *Classical and Quantum Gravity*, 27, 173001
- Abbott, B. P., Abbott, R., Abbott, T. D. et al. 2017, *PhRvL*, 119, 161101
- Abbott, B. P., Abbott, R., Abbott, T. D. et al. 2017, arXiv:1710.05838
- Abbott, B. P., Abbott, R., Abbott, T. D. et al. 2017, arXiv:1710.05836
- Abramowicz, M. A., Chen, X., Kato, S., Lasota, J.-P., & Regev, O. 1995, *ApJL*, 438, L37
- Alexander, K. D., Berger, E., Fong, W., et al. 2017, arXiv:1710.05457
- Aloy, M. A., Janka, H.-T., & Müller, E. 2005, *A&A*, 436, 273
- Amati, L., Guidorzi, C., Frontera, F., et al. 2008, *MNRAS*, 391, 577
- Amati, L., Frontera, F., & Guidorzi, C. 2009, *A&A*, 508, 173
- Antonelli, L. A., D'Avanzo, P., Perna, R., et al. 2009, *A&A*, 507, L45
- Bauswein, A., Goriely, S., & Janka, H.-T. 2013, *ApJ*, 773, 78
- Begelman, M. C. 2012, *MNRAS*, 420, 2912
- Berger, E., Fong, W., & Chornock, R. 2013, *ApJL*, 774, L23
- Berger, E., Zauderer, B. A., Levan, A., et al. 2013, *ApJ*, 765, 121
- Berger, E. 2014, *ARA&A*, 52, 43
- Blanchard, P. K., Berger, E., Fong, W., et al. 2017, *ApJL*, 848, L22
- Blandford, R. D., & Begelman, M. C. 1999, *MNRAS*, 303, L1
- Blandford, R. D., & Begelman, M. C. 2004, *MNRAS*, 349, 68
- Blandford, R. D., & McKee, C. F. 1977, *MNRAS*, 180, 343
- Blandford, R. D., & Payne, D. G. 1982, *MNRAS*, 199, 883
- Blandford, R. D., & Znajek, R. L. 1977, *MNRAS*, 179, 433
- Butler, N. R., Kocevski, D., Bloom, J. S., & Curtis, J. L. 2007, *ApJ*, 671, 656
- Burrows, D. N., Romano, P., Falcone, A., et al. 2005, *Science*, 309, 1833
- Campana, S., Mangano, V., Blustin, A. J., et al. 2006, *Nature*, 442, 1008
- Chawla, S., Anderson, M., Besselman, M., et al. 2010, *Physical Review Letters*, 105, 111101
- Cheung, E., Bundy, K., Cappellari, M., et al. 2016, *Nature*, 533, 504
- Chincarini, G., Mao, J., Margutti, R., et al. 2010, *MNRAS*, 406, 2113
- Chornock, R., Berger, E., Kasen, D., et al. 2017, arXiv:1710.05454
- Connaughton, V. 2002, *ApJ*, 567, 1028
- Cowperthwaite, P. S., Berger, E., Villar, V. A., et al. 2017, *ApJL*, 848, L17
- Cummings, J. R., Barthelmy, S. D., Baumgartner, W. H., et al. 2013, *GRB Coordinates Network*, 15293, 1
- Cutler, C., & Flanagan, É. E. 1994, *PhRvD*, 49, 2658
- Dai, Z. G., & Lu, T. 1998, *A&A*, 333, L87
- Dai, Z. G., Wang, X. Y., Wu, X. F., & Zhang, B. 2006, *Science*, 311, 1127
- Della Valle, M., Chincarini, G., Panagia, N., et al. 2006, *Nature*, 444, 1050
- Demianski, M., Piedipalumbo, E., Sawant, D., & Amati, L. 2017, *A&A*, 598, A112
- Dichiara, S., Guidorzi, C., Amati, L., Frontera, F., & Margutti, R. 2016, *A&A*, 589, A97
- Dietrich, T., Bernuzzi, S., Ujevic, M., & Brüggmann, B. 2015, *PhRvD*, 91, 124041
- Di Matteo, T., Perna, R., & Narayan, R. 2002, *ApJ*, 579, 706
- Eggum, G. E., Coroniti, F. V., & Katz, J. I. 1988, *ApJ*, 330, 142
- Eichler, D., Livio, M., Piran, T., & Schramm, D. N. 1989, *Nature*, 340, 126
- Evans, P. A., Cenko, S. B., Kennea, J. A., et al. 2017, arXiv:1710.05437
- Fan Y.-Z., & Wei D.-M. 2011, *ApJ*, 739, 47
- Fan, Y.-Z., Yu, Y.-W., Xu, D., et al. 2013, *ApJL*, 779, L25
- Fong, W., Berger, E., Blanchard, P. K., et al. 2017, arXiv:1710.05438
- Foucart, F., Deaton, M. B., Duez, M. D., et al. 2014, *PhRvD*, 90, 024026
- Fruchter, A. S., Levan, A. J., Strolger, L., et al. 2006, *Nature*, 441, 463
- Fynbo, J. P. U., Watson, D., Thöne, C. C., et al. 2006, *Nature*, 444, 1047
- Galama, T. J., Vreeswijk, P. M., van Paradijs, J., et al. 1998, *Nature*, 395, 670
- Gal-Yam, A., Fox, D. B., Price, P. A., et al. 2006, *Nature*, 444, 1053
- Gao, H., Ding, X., Wu, X.-F., Zhang, B., & Dai, Z.-G. 2013, *ApJ*, 771, 86
- Gao, H., Ding, X., Wu, X.-F., Dai, Z.-G., & Zhang, B. 2015, *ApJ*, 807, 163
- Gao, H., Ren, A.-B., Lei, W.-H., et al. 2017a, *ApJ*, 845, 51
- Gao, H., Zhang, B., Lü, H.-J., & Li, Y. 2017b, *ApJ*, 837, 50
- Gehrels, N., Norris, J. P., Barthelmy, S. D., et al. 2006, *Nature*, 444, 1044
- Ghirlanda, G., Nava, L., Ghisellini, G., et al. 2012, *MNRAS*, 420, 483
- Gorbovskoy, E. S., Lipunova, G. V., Lipunov, V. M., et al. 2012, *MNRAS*, 421, 1874
- Greiner, J., Krühler, T., Fynbo, J. P. U., et al. 2009, *ApJ*, 693, 1610
- Gu, W.-M. 2015, *ApJ*, 799, 71
- Gu, W.-M., & Lu, J.-F. 2007, *ApJ*, 660, 541
- Guidorzi, C., Clemens, C., Kobayashi, S., et al. 2009, *A&A*, 499, 439
- Guidorzi, C., Kobayashi, S., Perley, D. A., et al. 2011, *MNRAS*, 417, 2124
- Hallinan, G., Corsi, A., Mooley, K. P., et al. 2017, arXiv:1710.05435
- Hawley, J. F., Balbus, S. A., & Stone, J. M. 2001, *ApJL*, 554, L49
- Hjorth, J., Sollerman, J., Møller, P., et al. 2003, *Nature*, 423, 847
- Horesh, A., Hotokezaka, K., Piran, T., Nakar, E., & Hancock, P. 2016, *ApJL*, 819, L22
- Horváth, I. 2002, *A&A*, 392, 791
- Hotokezaka, K., Kiuchi, K., Kyutoku, K., et al. 2013, *PhRvD*, 87, 024001
- Igumenshchev, I. V., Narayan, R., & Abramowicz, M. A. 2003, *ApJ*, 592, 1042
- Janiuk, A., & Proga, D. 2008, *ApJ*, 675, 519
- Jiang, Y.-F., Stone, J. M., & Davis, S. W. 2014, *ApJ*, 796, 106
- Jiang, Y.-F., Stone, J. M., & Davis, S. W. 2017, arXiv:1709.02845
- Jin, Z.-P., Li, X., Cano, Z., et al. 2015, *ApJL*, 811, L22
- Jin, Z.-P., Hotokezaka, K., Li, X., et al. 2016, *Nature Communications*, 7, 12898
- Just, O., Bauswein, A., Pulpillo, R. A., Goriely, S., & Janka, H.-T. 2015, *MNRAS*, 448, 541
- Kann, D. A., Klose, S., Zhang, B., et al. 2010, *ApJ*, 720, 1513
- Kann, D. A., Klose, S., Zhang, B., et al. 2011, *ApJ*, 734, 96
- Kasliwal, M. M., Korobkin, O., Lau, R. M., Wollaeger, R., & Fryer, C. L. 2017, *ApJL*, 843, L34
- Kawaguchi, K., Kyutoku, K., Nakano, H., et al. 2015, *PhRvD*, 92, 024014
- Kawaguchi, K., Kyutoku, K., Shibata, M., & Tanaka, M. 2016, *ApJ*, 825, 52
- Kawanaka, N., Piran, T., & Krolik, J. H. 2013, *ApJ*, 766, 31
- Kilpatrick, C. D., Foley, R. J., Kasen, D., et al. 2017, arXiv:1710.05434
- Kisaka, S., Ioka, K., & Nakamura, T. 2015, *ApJL*, 809, L8

- Kiuchi, K., Sekiguchi, Y., Kyutoku, K., et al. 2015, *PhRvD*, 92, 064034
- Kouveliotou, C., Meegan, C. A., Fishman, G. J., et al. 1993, *ApJL*, 413, L101
- Krühler, T., Greiner, J., Afonso, P., et al. 2009, *A&A*, 508, 593
- Kulkarni, S. R. 2005, arXiv:astro-ph/0510256
- Kumar, P., & Zhang, B. 2015, *PhR*, 561, 1
- Kyutoku, K., Ioka, K., Okawa, H., Shibata, M., & Taniguchi, K. 2015, *PhRvD*, 92, 044028
- Laskar, T., Berger, E., Margutti, R., et al. 2015, *ApJ*, 814, 1
- Lazzati, D., Ramirez-Ruiz, E., & Ghisellini, G. 2001, *A&A*, 379, L39
- Lazzati, D., Deich, A., Morsony, B. J., & Workman, J. C. 2017, *MNRAS*, 471, 1652
- Lee, H. K., Brown, G. E., & Wijers, R. A. M. J. 2000a, *ApJ*, 536, 416
- Lee, H. K., Wijers, R. A. M. J., & Brown, G. E. 2000b, *PhR*, 325, 83
- Lei, W. H., Wang, D. X., Zhang, L., et al. 2009, *ApJ*, 700, 1970
- Lei, W.-H., Zhang, B., & Liang, E.-W. 2013, *ApJ*, 765, 125
- Lei, W.-H., Zhang, B., Wu, X.-F., & Liang, E.-W. 2017, arXiv:1708.05043
- Levan, A. J., Crowther, P., de Grijs, R., et al. 2016, *SSRv*, 202, 33
- Levesque, E. M., Bloom, J. S., Butler, N. R., et al. 2010, *MNRAS*, 401, 963
- Levesque, E. M., & Kewley, L. J. 2007, *ApJL*, 667, L121
- Li, L.-X., & Paczyński, B. 1998, *ApJL*, 507, L59
- Li, Y., Zhang, B., & Lü, H.-J. 2016, *ApJS*, 227, 7
- Lipunov, V. M., Postnov, K. A., & Prokhorov, M. E. 1997, *MNRAS*, 288, 245
- Liu, T., Gu, W.-M., Xue, L., Weng, S.-S., & Lu, J.-F. 2008, American Institute of Physics Conference Series, 1065, 298
- Liu, T., Gu, W.-M., Xue, L., & Lu, J.-F. 2007, *ApJ*, 661, 1025
- Liu, T., Gu, W.-M., Xue, L., & Lu, J.-F. 2012a, *Ap&SS*, 337, 711
- Liu, T., Gu, W.-M., Zhang, B. 2017a, *New Astronomy Reviews*, in press, arXiv:1705.05516
- Liu, T., Hou, S.-J., Xue, L., & Gu, W.-M. 2015a, *ApJS*, 218, 12
- Liu, T., Liang, E.-W., Gu, W.-M., et al. 2012b, *ApJ*, 760, 63
- Liu, T., Lin, Y.-Q., Hou, S.-J., & Gu, W.-M. 2015b, *ApJ*, 806, 58
- Liu, T., Lin, C.-Y., Song, C.-Y., & Li, A. 2017b, arXiv:1709.09810
- Liu, T., Song, C.-Y., Zhang, B., Gu, W.-M., & Heger, H. 2017c, *ApJ*, submitted
- Lü, H.-J., Zhang, B., Liang, E.-W., Zhang, B.-B., & Sakamoto, T. 2014, *MNRAS*, 442, 1922
- Lü, H.-J., Zhang, H.-M., Zhong, S.-Q., et al. 2017, *ApJ*, 835, 181
- Ma, S.-B., Lei, W.-H., Gao, H., et al. 2017, arXiv:1710.06318
- MacFadyen, A. I., & Woosley, S. E. 1999, *ApJ*, 524, 262
- Machida, M., Matsumoto, R., & Mineshige, S. 2001, *PASJ*, 53, L1
- Margutti, R., Berger, E., Fong, W., et al. 2017, *ApJL*, 848, L20
- Margutti, R., Guidorzi, C., Chincarini, G., et al. 2010, *MNRAS*, 406, 2149
- Marshall, F. E., Antonelli, L. A., Burrows, D. N., et al. 2011, *ApJ*, 727, 132
- McKinney, J. C., Tchekhovskoy, A., Sądowski, A., & Narayan, R. 2014, *MNRAS*, 441, 3177
- Metzger, B. D. 2017, *Living Reviews in Relativity*, 20, 3
- Metzger, B. D., & Berger, E. 2012, *ApJ*, 746, 48
- Metzger, B. D., & Fernández, R. 2014, *MNRAS*, 441, 3444
- Metzger, B. D., Martínez-Pinedo, G., Darbha, S., et al. 2010, *MNRAS*, 406, 2650
- Metzger, B. D., & Piro, A. L. 2014, *MNRAS*, 439, 3916
- Mu, H.-J., Gu, W.-M., Hou, S.-J., et al. 2016a, *ApJ*, 832, 161
- Mu, H.-J., Lin, D.-B., Xi, S.-Q., et al. 2016b, *ApJ*, 831, 111
- Nakamura, T., Kashiyama, K., Nakauchi, D., et al. 2014, *ApJ*, 796, 13
- Nakar, E. 2007, *PhR*, 442, 166
- Nakar, E., & Piran, T. 2011, *Nature*, 478, 82
- Narayan, R., Paczyński, B., & Piran, T. 1992, *ApJL*, 395, L83
- Narayan, R., Piran, T., & Kumar, P. 2001, *ApJ*, 557, 949
- Narayan, R., & Yi, I. 1994, *ApJL*, 428, L13
- Narayan, R., & Yi, I. 1995, *ApJ*, 444, 231
- Nemmen, R. S., Georganopoulos, M., Guiriec, S., et al. 2012, *Science*, 338, 1445
- Nicholl, M., Berger, E., Kasen, D., et al. 2017, arXiv:1710.05456
- Norris, J. P., Gehrels, N., & Scargle, J. D. 2010, *ApJ*, 717, 411
- Norris, J. P., Gehrels, N., & Scargle, J. D. 2011, *ApJ*, 735, 23
- Nousek, J. A., Kouveliotou, C., Grupe, D., et al. 2006, *ApJ*, 642, 389
- Oechslin, R., & Janka, H.-T. 2006, *MNRAS*, 368, 1489
- Oechslin, R., Janka, H.-T., & Marek, A. 2007, *A&A*, 467, 395
- Ofek, E. O., Cenko, S. B., Gal-Yam, A., et al. 2007, *ApJ*, 662, 1129
- Ohsuga, K., & Mineshige, S. 2011, *ApJ*, 736, 2
- Ohsuga, K., Mori, M., Nakamoto, T., & Mineshige, S. 2005, *ApJ*, 628, 368
- Okuda, T. 2002, *PASJ*, 54, 253
- Paczyński, B. 1986, *ApJL*, 308, L43
- Paczyński, B. 1991, *AcA*, 41, 257
- Pal'Shin, V., Golenetskii, S., Aptekar, R., et al. 2008, GRB Coordinates Network, 8256, 1
- Pang, B., Pen, U.-L., Matzner, C. D., Green, S. R., & Liebendörfer, M. 2011, *MNRAS*, 415, 1228
- Parker, M. L., Pinto, C., Fabian, A. C., et al. 2017a, *Nature*, 543, 83
- Parker, M. L., Alston, W. N., Buisson, D. J. K., et al. 2017b, *MNRAS*, 469, 1553
- Perley, D. A., Metzger, B. D., Granot, J., et al. 2009, *ApJ*, 696, 1871
- Pérez-Ramírez, D., de Ugarte Postigo, A., Gorosabel, J., et al. 2010, *A&A*, 510, A105
- Piran, T., Nakar, E., & Rosswog, S. 2013, *MNRAS*, 430, 2121
- Popham, R., Woosley, S. E., & Fryer, C. 1999, *ApJ*, 518, 356
- Racusin, J. L., Liang, E. W., Burrows, D. N., et al. 2009, *ApJ*, 698, 43
- Rhoads, J. E. 1999, *ApJ*, 525, 737
- Rossi, E. M., & Begelman, M. C. 2009, *MNRAS*, 392, 1451
- Rosswog, S. 2007, *MNRAS*, 376, L48
- Rowlinson, A., O'Brien, P. T., Metzger, B. D., Tanvir, N. R., & Levan, A. J. 2013, *MNRAS*, 430, 1061
- Ryan, G., van Eerten, H., MacFadyen, A., & Zhang, B.-B. 2015, *ApJ*, 799, 3
- Sądowski, A., & Narayan, R. 2015, *MNRAS*, 453, 3213
- Sądowski, A., Narayan, R., McKinney, J. C., & Tchekhovskoy, A. 2014, *MNRAS*, 439, 503
- Sakamoto, T., Barthelmy, S. D., Baumgartner, W. H., et al. 2014, GRB Coordinates Network, 16438, 1
- Savaglio, S., Glazebrook, K., & Le Borgne, D. 2009, *ApJ*, 691, 182
- Schutz, B. F. 1989, *Classical and Quantum Gravity*, 6, 1761
- Shappee, B. J., Simon, J. D., Drout, M. R., et al. 2017, *Shakura, N. I., & Sunyaev, R. A. 1973, A&A, 24, 337*
- Siegel, D. M., & Metzger, B. D. 2017, arXiv:1705.05473
- Smartt, S. J., Chen, T.-W., Jerkstrand, A., et al. 2017, arXiv:1710.05841
- Song, C.-Y., Liu, T., Gu, W.-M., & Tian, J.-X. 2016, *MNRAS*, 458, 1921
- Stanbro, M., & Meegan, C. 2016, GRB Coordinates Network, 19843, 1
- Stanek, K. Z., Matheson, T., Garnavich, P. M., et al. 2003, *ApJL*, 591, L17

- Stone, J. M., Pringle, J. E., & Begelman, M. C. 1999, *MNRAS*, 310, 1002
- Sun, H., Zhang, B., & Gao, H. 2017, *ApJ*, 835, 7
- Tanvir, N. R., Levan, A. J., Fruchter, A. S., et al. 2013, *Nature*, 500, 547
- Thompson, C. 1994, *MNRAS*, 270, 480
- Troja, E., Cusumano, G., O'Brien, P. T., et al. 2007, *ApJ*, 665, 599
- Troja, E., Piro, L., van Eerten, H., et al. 2017, arXiv:1710.05433
- Tsutsui, R., Yonetoku, D., Nakamura, T., Takahashi, K., & Morihara, Y. 2013, *MNRAS*, 431, 1398
- Tutukov, A. V., Yungelson, L. R., & Iben, I., Jr. 1992, *ApJ*, 386, 197
- Usov, V. V. 1992, *Nature*, 357, 472
- Wang, Q. D., Nowak, M. A., Markoff, S. B., et al. 2013, *Science*, 341, 981
- Wosley, S. E. 1993, *ApJ*, 405, 273
- Wosley, S. E., & Bloom, J. S. 2006, *ARA&A*, 44, 507
- Wu, X. F., Dai, Z. G., Wang, X. Y., et al. 2007, *Advances in Space Research*, 40, 1208
- Xiao, D., Liu, L.-D., Dai, Z.-G., & Wu, X.-F. 2017, arXiv:1710.05910
- Xin, L.-P., Liang, E.-W., Wei, J.-Y., et al. 2011, *MNRAS*, 410, 27
- Xu, D., Starling, R. L. C., Fynbo, J. P. U., et al. 2009, *ApJ*, 696, 971
- Yang, B., Jin, Z.-P., Li, X., et al. 2015, *Nature Communications*, 6, 7323
- Yasuda, T., Urata, Y., Enomoto, J., & Tashiro, M. S. 2017, *MNRAS*, 466, 4558
- Yi, S.-X., Xi, S.-Q., Yu, H., et al. 2016, *ApJS*, 224, 20
- Yu, Y.-W., Zhang, B., & Gao, H. 2013, *ApJL*, 776, L40
- Yuan, F., Bu, D., & Wu, M. 2012a, *ApJ*, 761, 130
- Yuan, F., & Narayan, R. 2014, *ARA&A*, 52, 529
- Yuan, F., Wu, M., & Bu, D. 2012b, *ApJ*, 761, 129
- Zaninoni, E., Bernardini, M. G., Margutti, R., & Amati, L. 2016, *MNRAS*, 455, 1375
- Zhang, B., & Mészáros, P. 2001, *ApJL*, 552, L35
- Zhang, B. 2013, *ApJL*, 763, L22
- Zhang, B., Liang, E., Page, K. L., et al. 2007a, *ApJ*, 655, 989
- Zhang, B., Zhang, B.-B., Liang, E.-W., et al. 2007b, *ApJL*, 655, L25
- Zhang, B., Zhang, B.-B., Virgili, F. J., et al. 2009, *ApJ*, 703, 1696
- Zhang, B.-B. 2011, Ph.D. Thesis
- Zhang, B.-B., Zhang, B., Murase, K., Connaughton, V., & Briggs, M. S. 2014, *ApJ*, 787, 66
- Zhang, B.-B., Zhang, B., Sun, H., et al. 2017, arXiv:1710.05851
- Zhang, F.-W., Shao, L., Yan, J.-Z., & Wei, D.-M. 2012, *ApJ*, 750, 88